

Hydrostatic pressure effects on the dielectric response of potassium cyanide

JAIME ORTIZ LÓPEZ*

Escuela Superior de Física y Matemáticas

Instituto Politécnico Nacional

Edif. 9, U.P.A.L.M., 07738 México, D.F., México

Recibido el 26 de mayo de 1992; aceptado el 10 de julio de 1992

ABSTRACT. The complex dielectric constant of crystalline KCN was measured under hydrostatic pressures up to 6.1 kbar in the temperature and frequency ranges of 50–300 K and $10\text{--}10^5$ Hz, respectively. It is found that the pressure derivative of the real part of the dielectric constant at all measured temperatures is negative. From these results we obtain estimates for the pressure and volume derivatives of polarizabilities. The anomaly in the real part of the dielectric constant at the elastic order-disorder transition shifts to higher temperatures with increasing pressure at a rate of 2.05 K/kbar. By carefully avoiding thermal cycling through this transition we find no evidence of the monoclinic phase reported to exist in the P - T phase diagram of KCN at relatively low pressures. Dielectric loss measurements show thermally-activated CN^- reorientation rates in the elastically ordered phase with pressure-independent reorientational barriers and decreasing attempt frequencies for increasing pressures. Additional pressure effects on dielectric loss allow to obtain the pressure derivative of the antiferroelectric transition temperature as 1.97 K/kbar.

RESUMEN. Se midió la constante dieléctrica compleja de KCN cristalino bajo presiones hidrostáticas de hasta 6.1 kbar en el rango de temperaturas 50–300 K y de frecuencias $10\text{--}10^5$ Hz. Se encuentra que la derivada de la parte real de la constante dieléctrica respecto de la presión es negativa en todo el rango de temperaturas medido. De estos resultados se obtienen estimaciones de las derivadas de las polarizabilidades respecto de la presión y del volumen. La anomalía de la parte real de la constante dieléctrica en la transición elástica orden-desorden, se desplaza hacia altas temperaturas al aumentar la presión a razón de 2.05 K/kbar. Evitando cuidadosamente el ciclamiento térmico alrededor de esta transición, no se encuentra evidencia de la fase monoclinica que se ha reportado existir en el diagrama P - T de KCN a presiones relativamente bajas. Mediciones de pérdida dieléctrica muestran que la reorientación de los iones moleculares CN^- es térmicamente activada en la fase elásticamente ordenada, con barreras orientacionales independientes de la presión y frecuencias de intento que decrecen con la presión. Interpretación de efectos adicionales de la presión sobre la pérdida dieléctrica permiten obtener la derivada respecto de la presión de la temperatura de transición antiferroeléctrica con un valor de 1.97 K/kbar.

PACS: 62.50.+p; 77.20.+y; 77.40.+i

1. INTRODUCTION

The alkali cyanides have long been considered as model cases of a large group of ionic crystals with general composition $\text{M}^+(\text{XY})^-$ which show interesting collective phenomena

*Becario COFAA-IPN.

due to interactions between the $(XY)^-$ radicals [1]. Because of the rapid rotation of the CN^- molecular ion at high temperatures and atmospheric pressure, the alkali cyanides show pseudocubic structures similar to those of the corresponding alkali halides [2-5]. In this temperature regime, the alkali halide KBr is the closest analog to KCN in terms of lattice constant size. Under cooling, transitions into different orientationally ordered phases occur induced by the collective ordering of the CN^- ions. At $T_{c1} = 168$ K for KCN at atmospheric pressure, the CN^- ions assume, in a first-order *ferroelastic* phase transition, a parallel arrangement which produces a shearing and uniaxial contraction of the cubic cell leading to an orthorhombic structure [6-9]. The ferroelastic nature of this transition stems from the fact that, due to its shape—an approximate ellipsoid with 2.2 and 1.8 Å semiaxes—the CN^- ion produces *elastic* distortions in the lattice that can be treated by an *elastic dipole* model [10,11]. The transition to a parallel arrangement of these elastic dipoles then resembles ferromagnetic ordering. In this elastically ordered phase, the CN^- ions are aligned close to the six [10] directions of the original cubic cell but remain disordered in terms of the direction of their permanent electric dipole moment (space group Immm). This electric disorder is gradually removed below $T_{c2} = 83$ K, at atmospheric pressure, in a second-order phase transition leading eventually to a fully ordered (layered) antiferroelectric structure (space group Pmmn) [8,9]. Besides this “normal” order-disorder behavior of KCN at atmospheric pressure, an additional metastable intermediate monoclinic phase (space group Aa) may exist in a narrow temperature range just below 167 K if the crystal is subjected to thermal cycling around T_{c1} [12-15].

The dielectric response of KCN at atmospheric pressure is well characterized [16-18]. Under cooling from room temperature, the real part $\epsilon'(T)$ of the dielectric constant of KCN decreases with a temperature slope similar to that of KCl (the value of ϵ' at room temperature being larger for KCN). At $T_{c1} = 168$ K a sharp and frequency-independent decrease in $\epsilon'(T)$ announces the ferroelastic phase transition with no observable dielectric losses. With further cooling, $\epsilon'(T)$ keeps decreasing with a KCl-like temperature slope, even down to the critical temperature of the antiferroelectric transition $T_{c2} \approx 83$ K, with no signs of any Curie or Curie-Weiss law behavior occurring [16]. In the range of 100-50 K and for frequencies between 10^2 - 10^5 Hz, $\epsilon'(T)$ decreases in a frequency-dependent way, accompanied by the appearance of (Kramers-Kronig) related Debye-type dielectric loss peaks due to slowing-down of CN^- dipolar reorientation. The reorientation of CN^- in this regime is thermally activated and well described by an Arrhenius-law behavior. In a log-frequency plot of dielectric loss, the peaks decrease in size (area) with decreasing temperature, reflecting a decrease in dipolar susceptibility caused by gradual alignment of CN^- dipoles due to antiferroelectric ordering below T_{c2} [16]. Further cooling below 50 K, brings $\epsilon'(T)$ of KCN close to that of KCl, both in value and temperature slope.

The P - T phase diagram of KCN has been investigated by the use of several experimental techniques in conjunction with the application of hydrostatic pressure [19-27]. According to some workers, it is only above 20 kbar when new high-pressure phases appear differing from those already present at atmospheric pressure [19-22]. Other workers, however, have found experimental evidence of a more complicated P - T phase diagram at lower pressures in which a neighboring monoclinic phase (related to the metastable one found by thermal cycling) exist, giving rise to a triple point located near 170 K and 0.3 kbar [23-26.]

Previously, dielectric studies on KCN under hydrostatic pressure have been done up to 7 kbar but only at a fixed temperature of 293.2 K, thus missing the observation of interesting pressure effects on the CN^- collective ordering behavior under cooling [28]. In this work our main goal is to study effects of hydrostatic pressure (up to 6 kbar) on the dielectric response of KCN under temperature and frequency variations. This allows us to obtain good estimates of pressure coefficients for the critical temperatures T_{c1} and T_{c2} and for the real part of the dielectric constant. Particular attention is paid to the analysis of the pressure dependence of CN^- reorientation as obtained from our dielectric loss measurements and to the reported existence of a monoclinic phase in the P - T phase diagram of KCN at relatively low pressures [23-26].

2. EXPERIMENTAL DETAILS

Pure KCN crystals were obtained from the University of Utah Crystal Growth Laboratory. The crystals were grown from the melt under argon atmosphere and using zone-refined material. Samples were cleaved and sanded to dimensions 0.45 mm \times 10 mm \times 12 mm and prepared with evaporated gold electrodes on each side. Very thin copper wires for electrical connections were glued to the electrodes with silver paint. The samples were mounted inside a cylindrical (1.5" diameter, 2.75" length) pressure cell constructed from maraging steel (Vascomax 300) having two electrical feedthroughs and high-pressure tubing connections to the pressurizing system. Sample preparation and handling was done under optimal dry conditions since KCN is hygroscopic.

Helium gas was used as the pressure transmitting medium. Pressure was generated in two stages. The first stage compressed bottled helium to 2 kbar with an air driven oil pump and separator. In the second stage an electrically driven oil pump generated up to 1 kbar of oil pressure to drive a Harwood intensifier to compress the 2 kbar gas to a maximum of 7-8 kbar in the best conditions of operation. Pressure was measured with a manganin cell with an accuracy of about 0.2%. The solidification point of He was never crossed during our experiments since temperatures were above 50 K and pressures below 6 kbar. The pressure cell was cooled inside a gas flow cryostat (Janis Super Vari-Temp 10DT). Sample temperature was measured with silicon diodes mounted outside the pressure cell at positions chosen to optimize thermal coupling between sample and temperature sensors. Temperature measurement and control was electronically achieved with a temperature indicator/controller (Lake Shore DTC-500). Temperature accuracy above 50 K is of about ± 1 K and of about ± 2 K near room temperature. To avoid He gas leaks through the pressure cell gaskets due to thermal effects during experimental runs, measurements under pressure were performed first and measurements at atmospheric pressure were performed last.

Real and imaginary parts of the dielectric constant were determined by capacitance/conductance measurements with a high precision three-terminal transformer ratio-arm bridge (General Radio 1621) at frequencies ranging between 10 Hz and 100 kHz and voltages within 1.5 and 15 V.

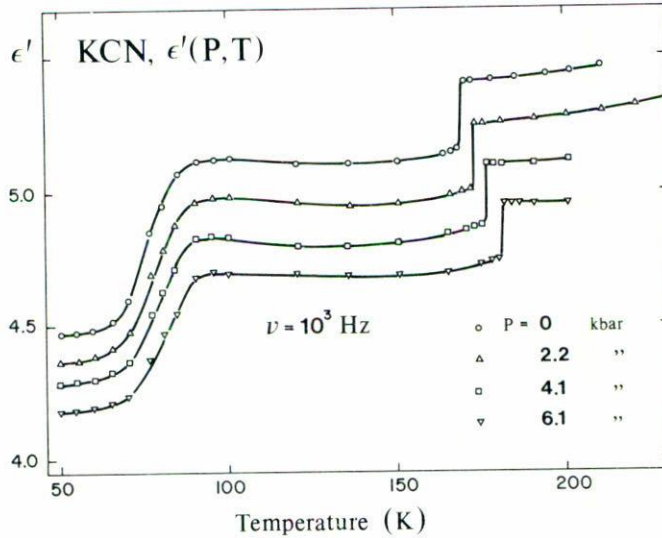


FIGURE 1. Temperature dependence of the real part of the dielectric constant at 1 kHz for several applied pressures.

3. RESULTS

In Fig. 1 we display for a single sample the measured real part of the dielectric constant $\epsilon'(P, T)$ at a frequency of 1 KHz as a function of temperature for three different applied pressures. For these measurements, temperature and pressure variations were carefully performed in order to avoid thermal cycling around the elastic phase transition, which is known to induce the formation of an intermediate metastable monoclinic ordered phase [12-15].

Under hydrostatic pressures up to 6.1 kbar, all the temperature-dependent features of ϵ' at atmospheric pressure ($P = 0.001 \text{ kbar} \approx 0 \text{ kbar}$) described in section 1 are present. No indications of the presence of an additional phase is detected at any pressure. The following pressure-induced changes are readily observed in Fig. 1: i) The $\epsilon'(P, T)$ curves shift to decreasing values as pressure is increased; ii) the anomaly in ϵ' at the critical temperature of the elastic order disorder phase transition ($T_{c1} = 168 \text{ K}$ for $P = 0 \text{ kbar}$) shifts linearly to higher temperatures with increasing pressure and; iii) the temperature region (70-100 K for $P = 0 \text{ kbar}$) in which the low-temperature gradual decrease of ϵ' takes place, slightly shifts to higher temperatures as pressure increases.

The first effect is common to normal ionic crystals like the alkali halides and indicates that the first-order pressure coefficient for $\epsilon'(T)$ is negative for all measured temperatures. Our data allows to obtain approximate values for this coefficient at particular temperatures as shown in the fourth column of Table I. The remaining data in Table I will be discussed later in Sect. 4.

The second effect shows that the pressure coefficient for T_{c1} is positive with a value of $2.05 \pm 0.03 \text{ K/kbar}$ according to our data. This value is in good agreement with results obtained with other experimental techniques [19-27].

The last effect is best seen in the same temperature range in terms of the associated

TABLE I. Temperature dependence of static ϵ_s and infrared ϵ_∞ dielectric constants, of their pressure derivatives and of the volume dependence of various contributions to the polarizability α for KCN. α_o , α_i and α_d , optical, infrared and dipolar macroscopic polarizabilities. Units: 10^{-4} kbar $^{-1}$ for pressure derivatives of dielectric constants; the remaining quantities are dimensionless. The values for ϵ_∞ and its pressure derivative are actually those for KCl reported in Ref. [29], and are taken as estimates for corresponding values for KCN (see discussion in Sect. 4).

Phase	T (K)	ϵ_s	$\left[\frac{\partial \ln \epsilon_s}{\partial P}\right]_T$	ϵ_∞^\ddagger	$\left[\frac{\partial \ln \epsilon_\infty}{\partial P}\right]_T^\ddagger$	$\left[\frac{\partial \ln \alpha}{\partial \ln V}\right]_T = \frac{\alpha_o}{\alpha} \left[\frac{\partial \ln \alpha_o}{\partial \ln V}\right]_T^* + \frac{\alpha_i}{\alpha} \left[\frac{\partial \ln \alpha_i}{\partial \ln V}\right]_T + \frac{\alpha_d}{\alpha} \left[\frac{\partial \ln \alpha_d}{\partial \ln V}\right]_T$
Fm 3m	293	5.60 [†]	-198 [†]	4.860	-126	2.29 = 0.41(1.12) + 0.52(2.57) + 0.07(7.06)
	190	5.38	-145	4.709	-111	1.98 = 0.42(1.12) + 0.51(2.50) + 0.07(3.35)
Immm	150	5.10	-143	4.656	-107	2.02 = 0.43(1.12) + 0.52(2.43) + 0.05(5.49)
	130	5.08	-140	4.630	-104	2.00 = 0.43(1.12) + 0.52(2.38) + 0.05(5.61)
	110	5.06	-135	4.607	-102	1.97 = 0.43(1.12) + 0.51(2.36) + 0.05(5.69)
Pmmn	80	4.97	-156	4.571	-100	2.14 = 0.44(1.12) + 0.52(2.37) + 0.04(10.37)
	70	4.82	-141	4.560	-100	2.06 = 0.44(1.12) + 0.53(2.36) + 0.03(10.54)

[†] Room temperature values from Ref. [28].

[‡] Values for KCl reported in Ref. [29].

*From Ref. [30].

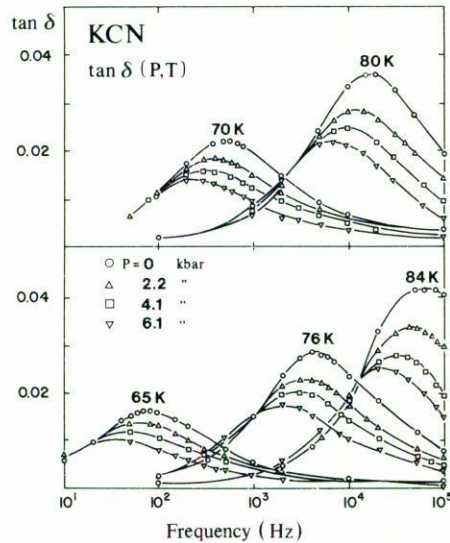


FIGURE 2. Log-frequency plots of dielectric loss $\tan \delta$ for KCN at selected temperatures and pressures.

dielectric loss $\tan \delta$ which is related to the imaginary part ϵ'' of the dielectric constant by: $\tan \delta = \epsilon''/\epsilon'$. In Fig. 2 we show log-frequency plots of $\tan \delta$ for selected temperatures and pressures. At any constant pressure, Debye-like peaks are detected in the 65–84 K temperature range within our experimental frequency window, which shift to lower frequencies and decrease in size (area) as temperature decreases. As described already in Sec. 1, the shift of the peaks is due to CN^- reorientation slowing-down and the decrease in size is due to gradual antiferroelectric ordering. The loss peaks are, in average, about 40% wider than ideal (single-relaxation) Debye peaks. The effect of pressure is best seen by looking the peaks at constant temperature and noting that increasing pressure causes: a) small shifts of the peaks towards lower frequency and, b) reductions in the peak sizes. The frequency of the peak centers ν_{\max} is related to the mean CN^- reorientation rate τ^{-1} by the relation: $\tau^{-1} = 2\pi\nu_{\max}$, where τ is the CN^- relaxation time. At constant pressure, the temperature-dependent frequency shift of the peaks can be fitted to an Arrhenius law

$$\tau^{-1}(P, T) = \nu_0(P) \exp[-U(P)/k_B T], \quad (1)$$

where $\nu_0(P)$ is a pressure-dependent attempt frequency; $U(P)$ is a pressure-dependent activation energy for reorientation and k_B is Boltzmann's constant. Least-square fits to our experimental data shown in Fig. 3 give the values of Table II. The results obtained for $P = 0$ kbar are slightly different from previously reported values [16] but our measurements are more accurate [1,17]. As the table shows, the attempt frequency decreases with pressure and, within experimental error, the reorientation energy remains constant.

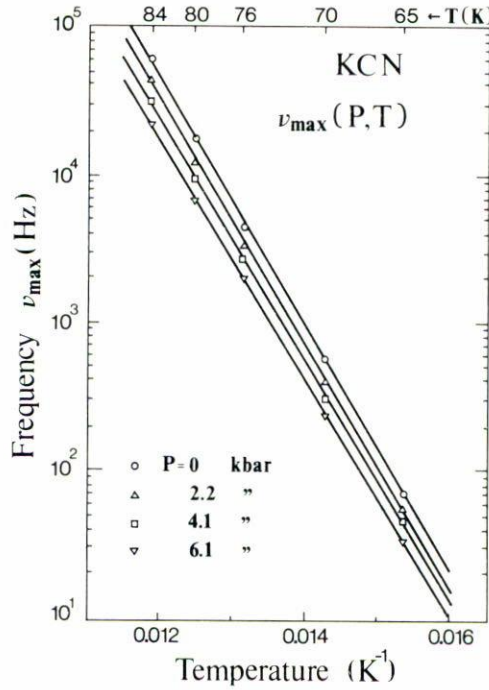


FIGURE 3. Arrhenius plot for the loss peaks positions at different pressures.

TABLE II. Pressure dependence of CN⁻ reorientation measured by dielectric loss in KCN.

Pressure <i>P</i> (kbar)	Attempt frequency $\nu_0(P)$ ($\times 10^{15} \text{ sec}^{-1}$)	Reorientation Energy $U(P)$ (meV)
0	5.057	0.157 ± 0.003
2.2	0.604	0.158 ± 0.003
4.1	0.394	0.156 ± 0.006
6.1	0.312	0.157 ± 0.003

4. DISCUSSION

4.1 Real part of the dielectric constant and the ferroelastic transition

The decrease of the $\epsilon'(P, T)$ curves with pressure in the whole temperature range, shows that the polarizabilities of all types (dipolar + ionic + electronic) in KCN have a decreasing pressure dependence which dominates over a possible increase in ϵ' due to a pressure-induced rise in the density of polarizable particles. This can be seen from the

following equation obtained from the Clausius-Mossotti relation [28]:

$$\begin{aligned} \left(\frac{\partial \ln \epsilon_s}{\partial P} \right)_T &= q \left[k + \left(\frac{\partial \ln \alpha}{\partial P} \right)_T \right] \\ &= qk \left[1 - \left(\frac{\partial \ln \alpha}{\partial \ln V} \right)_T \right], \end{aligned} \quad (2)$$

where ϵ_s is the static dielectric constant; $q = (\epsilon_s - 1)(\epsilon_s + 2)/3\epsilon_s$; $k = -(\partial \ln V/\partial P)$ is the isothermal volume compressibility and $\alpha = \alpha_o + \alpha_i + \alpha_d$ is the total polarizability composed of the optical (o), infrared (i) and dipolar (d) contributions. According to Julian's observations [16], the dielectric constant of KCN is essentially KCl-like with an additional dipolar contribution due to the orientational polarization of CN^- molecules modulated by their collective interactions. The rotational motions of the CN^- are coupled to the lattice modes in such a strong way [27] that the temperature slope of ϵ' in KCN is very similar to that of KCl, inhibiting any Curie or Curie-Weiss law behavior of the CN^- orientational polarizability. The above observations suggest that the orientational contribution of the CN^- can be extracted from the total polarizability by assuming that the rest of the polarizability $\alpha - \alpha_d$ is KCl-like. In order to do this, we can use the macroscopic Clausius-Mossotti relation in the following forms:

$$\begin{aligned} \frac{\epsilon_s - 1}{\epsilon_s + 2} &= \frac{4\pi}{3}(\alpha_o + \alpha_i + \alpha_d), \\ \frac{\epsilon_\infty - 1}{\epsilon_\infty + 2} &= \frac{4\pi}{3}(\alpha_o + \alpha_i), \\ \frac{\epsilon_o - 1}{\epsilon_o + 2} &= \frac{4\pi}{3}(\alpha_o), \end{aligned} \quad (3)$$

where ϵ_∞ is the dielectric constant at (infrared) frequencies for which the dipolar orientational polarization no longer contributes; ϵ_o is the dielectric constant at optical frequencies (which is equal to n^2 , with n the refraction index) and V is the volume of a macroscopic small sphere. The rest of the quantities in Eqs. (3) have the same meaning as before. By manipulating these three equations, the contribution of each component of the polarizability can be isolated. The pressure derivative of each of these components is thus related to the pressure derivatives of ϵ_o , ϵ_∞ and ϵ_s . Values for ϵ_s and its pressure derivative as a function of temperature obtained in this work are listed in Table I. For ϵ_∞ and its pressure derivative, we take in Table I values for KCl in Ref. [29] as an estimation of actual values for KCN. Data for ϵ_o and its pressure derivative for KCN are available only at room temperature [30] and have values of 1.99 and $-5.96 \times 10^{-4} \text{ kbar}^{-1}$, respectively. The bulk compressibility k of KCN is also available [30] only at room temperature and has a value of $73.6 \times 10^{-4} \text{ kbar}^{-1}$ at 0 kbar. With these data we obtain in Table I estimates for the volume derivatives of the various contributions to the polarizability as a function of temperature. For each species, these volume derivatives are related to the pressure derivatives by $(\partial \ln \alpha/\partial P)_T = -k(\partial \ln \alpha/\partial \ln V)_T$ as can be seen from Eq. (2). Some caution

should be taken with direct interpretation of the values shown in Table I since several oversimplifications have been made in their calculation. Perhaps the most restrictive one is the use of the Clausius-Mossotti relationship for the orthorhombic phases since this relationship is valid only for cubic crystals. Other simplifications are the use of room temperature values for ϵ_0 and its pressure derivative and for the compressibility k , due to the lack of numerical values for lower temperatures in the literature. Therefore the values in Table I should be taken as first approximations to the actual ones and should serve only to the purpose of getting their order of magnitude. With this in mind, it is remarkable that the temperature dependence displayed by the relative values of the various contributions is very reasonable. In particular, the disappearance of the dipolar contribution and the concomitant increase of the other contributions with lowering temperature is something to be expected in the range of the Pmmn phase due to antiferroelectric ordering. In crossing the ferroelastic transition, the relative contributions of all species of polarizability suffer a strong variation mainly due to the discontinuous decrease in static dielectric constant at the transition. The only two contributions whose volume derivatives satisfy Jarman's rule [28] are the total and infrared polarizabilities; the volume derivatives of the dipolar polarizability attain extremely high values in comparison.

The observed linear dependence of the transition temperature T_{c1} with pressure describes, at least up to 6 kbar, a linear phase boundary between the cubic (Fm 3m) and orthorhombic (Immm) phases in the P - T phase diagram of KCN having the form: $T_{c1}(P) = 167.5 \text{ K} + (2.05 \text{ K/kbar})P$. This linear dependence of T_{c1} on pressure is consistent with the idea of ferroelastic ordering of CN^- elastic dipoles [31].

4.2 Dielectric loss and the antiferroelectric phase transition

In regard to the two pressure effects observed in our dielectric loss measurements, these can be understood as follows.

a) The pressure-induced shifts of the peaks towards low frequency at any constant temperature are a manifestation of the decreasing rotational motions of the CN^- molecules with increasing pressure. The results of Table II give quantitative account of this effect. At constant temperature and increasing pressure, the reorientation rate decreases or, equivalently, the relaxation time increases. Pressure therefore inhibits the rotation of the CN^- molecules due to lattice compression. The pressure derivative of the relaxation time τ defines an activation volume ΔV^* through the relation [32]

$$\left(\frac{\partial \ln \tau}{\partial P} \right)_T = \frac{\Delta V^*}{RT}, \quad (4)$$

where R is the universal gas constant. This activation volume is positive according to our results and can be understood as the required volume expansion needed to accommodate the reorientation of the CN^- molecules. Our data yields decreasing values of ΔV^* from $0.502 \text{ cm}^3/\text{mole}$ (0.834 \AA^3) at 84 K to $0.27 \text{ cm}^3/\text{mole}$ (0.448 \AA^3) at 65 K. These values are small in comparison to the volumes of the (orthorhombic) unit cell and of the CN^- molecule (132 \AA^3 and 5.57 \AA^3 , respectively). Since increasing pressure compresses the lat-

tice, it becomes increasingly difficult for this volume expansion for CN^- reorientation to take place.

b) The pressure-induced reduction in peak sizes (at any constant temperature) can be understood by the critical temperature of the antiferroelectric phase transition T_{c2} being shifted towards higher temperature with increasing pressure. As we have previously mentioned, at any constant pressure the decrease in size (area) of the observed loss peaks is due to a gradual disappearance of field-alignable CN^- dipoles due to antiferroelectric ordering below T_{c2} . At a given temperature, reduction in peak size with pressure of the observed magnitude, can only be accounted for by a pressure-induced decrease in the number of dipoles participating in reorientation since it is unlikely that their permanent dipole moment could be greatly affected by the applied pressures. This possibility can be accomplished by a pressure-induced shift of the antiferroelectric phase transition temperature T_{c2} towards higher values. In order estimate the pressure coefficient of T_{c2} , we apply a simplified antiferroelectric model by Kittel [33] to our dielectric loss data. This model predicts a continuous variation of ϵ' through the antiferroelectric phase transition temperature if the transition is second-order as it occurs for KCN [18]. This model gives for the static susceptibility χ below T_{c2} :

$$\chi^{-1}(T) = \chi^{-1}(T_{c2}) + 2\lambda(T_{c2} - T), \quad (5)$$

where λ is a parameter which depends on the crystalline structure. The static susceptibility χ can be obtained from the integrated area of the loss peaks and the Kramers-Krönig relations in the form

$$\chi = 1.46(4\pi)\epsilon_{\infty}A, \quad (6)$$

where ϵ_{∞} is the high-frequency (infrared) dielectric constant, and A is the area under a dielectric loss peak in a \log_{10} -frequency plot. By manipulating our data we obtain the plot of Fig. 4(a) in which we show χ^{-1} as a function of temperature for different applied pressures. It is seen that the model reasonably fits our data. If we take into account the pressure decrease of ϵ' from Fig. 1, we find that the pressure-induced increase in χ^{-1} by only this cause is smaller than the one observed in Fig. 4(a). Therefore, the additional increase must come from a variation of T_{c2} with pressure. Assuming that λ does not change with pressure, we obtain the pressure dependence of T_{c2} shown in Fig. 4(b). A least-square fit to these results then gives a pressure coefficient of 1.97 ± 0.13 K/kbar, which is in good agreement with results obtained with other techniques [23]. The phase boundary separating the Immm and Pmmn orthorhombic phases in the P - T phase-diagram of KCN therefore can be described by the linear relation: $T_{c2}(P) = 88.86 \text{ K} + (1.97 \text{ K/kbar})P$, if we assume a $T_{c2} = 89$ K at atmospheric pressure [16,18].

4.3 The P - T phase diagram of KCN

According to the work of Dultz *et al.* [23,25], a triple point in the P - T phase diagram of KCN exists around 170 K and 0.3 kbar formed between the cubic (Fm 3m), orthorhombic (Immm) and a high-pressure monoclinic (A2/m) phases; the latter being related to the

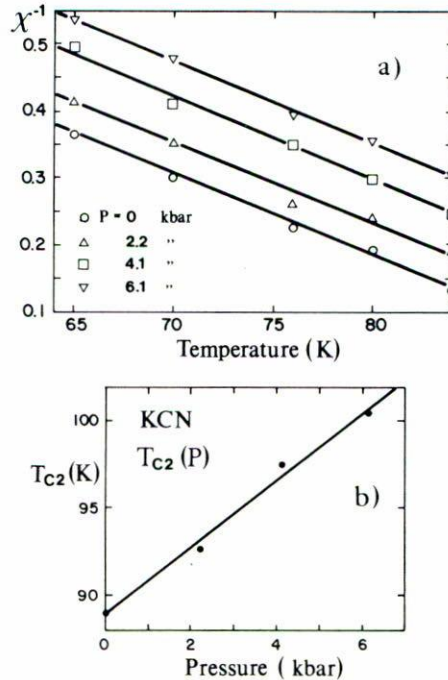


FIGURE 4. a) Integrated dielectric loss data fitted to the antiferroelectric model of Eq. (5). Solid lines are least-square fits; b) Pressure dependence of the antiferroelectric phase transition temperature T_{c2} derived from the model. Solid line is a least-squares fit.

one created by thermal cycling around T_{c1} at atmospheric pressure [12–15]. In our measurements of Fig. 1, however, we find no evidence of such a monoclinic phase reflected in the behavior of $\epsilon'(P, T)$. Evidence of an intermediate phase is indeed detected in ϵ' at atmospheric pressure produced by thermal cycling and observed as depression in the normal $\epsilon'(T)$ curve below T_{c1} whose temperature width depends on thermal history [14]. Not even traces of a similar behavior is detected in our results under hydrostatic pressure. Two possible explanations for this discrepancy can be formulated: 1) during the experiments of Dultz *et al.*, thermal cycling through T_{c1} was not avoided so that the reported monoclinic phase was actually created by thermal cycling and not by pressure; or 2) the dielectric technique is not sensible enough to detect the high-pressure monoclinic phase. In relation to the first possibility, it is unfortunate that nowhere in Dultz *et al.* papers is ever mentioned if they avoided or not thermal cycling. In our case, we were careful in this respect and we find no evidence of the monoclinic phase. Our results, in any case, are closer to those reported by Pistorius *et al.* [19–21] who did not detect such a phase. On the other hand, the second possibility seems unlikely since the monoclinic phase created by thermal cycling is clearly detected [14] in $\epsilon'(T)$ and we find no reason for this not to happen with the one created by pressure. Still, it appears difficult to abandon the idea of a triple point existing at relatively low pressures since this explains in a natural way the appearance of the monoclinic phase created by thermal cycling [14]. Unfortunately at this stage we are not able to confirm it on the basis of the present results.

ACKNOWLEDGMENTS

All reported experiments were performed at the University of Utah. I would like to thank Professor Fritz Luty for many helpful and enlightening discussions.

REFERENCES

1. F. Luty in *Defects in Insulating Crystals*, edited by V.M. Turkevich and K.K. Shvarts, Springer-Verlag, Berlin (1981) pp. 69-89.
2. D.L. Price, J.M. Rowe, J.J. Rush, E. Prince, D.G. Hinks, and S. Susman, *J. Chem. Phys.* **56** (1972) 3697.
3. E.O' Reilly, E.M. Peterson, C.E. Scheie and P.K. Kadaba, *J. Chem. Phys.* **58** (1973) 3018.
4. S. Haussühl, *Solid State Commun.* **13** (1973) 147.
5. R.E. Wasylishen, B.A. Pettitt and K.R. Jeffrey, *J. Chem. Phys.* **74** (1981) 6022.
6. J.M. Bijvoet and J.A. Lely, *Rec. Trav. Chim. Pays Bas* **59** (1940) 908.
7. H. Suga, T. Matsuo, S. Seki, *Bull. Chem. Soc. Jpn.* **38** (1965) 1115.
8. J.M. Rowe, J.J. Rush and E. Prince, *J. Chem. Phys.* **66** (1977) 5147.
9. D. Fontaine, *C.R. Acad. Sci. (Paris)* **B281** (1975) 443.
10. A.S. Nowick and W.R. Heller, *Adv. Phys.* **12** (1973) 147.
11. Z. Yang and F. Luty, *Phys. Status Solidi (b)* **154** (1989) 167.
12. A. Cimino, G.S. Parry, and A.R. Ubbelohde, *Proc. R. Soc. London* **A252** (1959) 445.
13. G.S. Parry, *Acta Crystallogr.* **15** (1962) 601.
14. J. Ortiz-Lopez and F. Luty, *Phys. Rev.* **B37** (1988) 5452.
15. Y. Yoshimura and K. Shimaoka, *J. Phys. Soc. Jpn.* **57** (1988) 3052.
16. M. Julian and F. Luty, *Ferroelectrics* **16** (1977) 201; M.D. Julian, *Ph.D. Thesis*, University of Utah (1976).
17. F. Luty and J. Ortiz-Lopez, *Phys. Rev. Lett.* **50** (1983) 1289.
18. B. Koiller, M.A. Davidovich and F. Luty, *Phys. Rev.* **B31** (1985) 6716.
19. C.W.F.T. Pistorius, *Progr. in Solid State Chemistry* **11** (1976) 1.
20. C.W.F.T. Pistorius, J.B. Clark and E. Rapoport, *J. Chem. Phys.* **48** (1968) 5123.
21. P.W. Richter and C.W.F.T. Pistorius, *Acta Crystallogr.* **B28** (1972) 3105.
22. D.L. Decker, R.A. Beyerlein, G. Roullet, and T.G. Worlton, *Phys. Rev.* **B10** (1974) 3584.
23. W. Dultz and H. Krause, *Phys. Rev.* **B18** (1978) 394.
24. M. Stock and W. Dultz, *Phys. Status Solidi(a)* **53** (1979) 237.
25. W. Dultz, H.H. Otto, H. Krause and J.L. Buevoz, *Phys. Rev.* **B24** (1987) 1287.
26. K. Strössner, H.D. Hochheimer, W. Hönle and A. Werner, *J. Chem. Phys.* **83** (1985) 2435.
27. H.D. Hochheimer, W.F. Love and C.T. Walker, *Phys. Rev. Lett.* **38** (1977) 832.
28. P. Preu and S. Haussühl, *J. Phys. Chem. Solids* **46** (1985) 265.
29. R.A. Bartels and P.A. Smith, *Phys. Rev.* **B7** (1973) 3885.
30. Landolt-Börnstein, *Numerical Data and Functional Relationships in Science and Technology*, 6th Edition II/8 (1962) and New Series III/11 (1979). Springer-Verlag, Berlin.
31. Z. Yang, J. Ortiz-Lopez and F. Luty, *Phys. Status Solidi (b)* **159** (1990) 629.
32. E. Whalley in *Advances in High Pressure Research*, Vol. 1 (1966).
33. C. Kittel, *Phys. Rev.* **82** (1951) 729.